CHINESE OPTICS LETTERS

Vol. 19, No. 7 | July 2021

Optical resonance in inhomogeneous parity-time symmetric systems

Linshan Sun (孙林山)[1,†], Bo Zhao (赵 博)[1,†], Jiaqi Yuan (袁家琪)[1,†], Yanrong Zhang (张艳荣)[1], Ming Kang (康 明)[2], and Jing Chen (陈 璟)[1,3*]

[1] MOE Key Laboratory of Weak-Light Nonlinear Photonics, School of Physics, Nankai University, Tianjin 300071, China

[2] College of Physics and Materials Science, Tianjin Normal University, Tianjin 300387, China

[3] Collaborative Innovation Center of Extreme Optics, Shanxi University, Taiyuan 030006, China

*Corresponding author: jchen4@nankai.edu.cn

Received October 29, 2020 | Accepted December 19, 2020 | Posted Online March 22, 2021

We show that inhomogeneous waveguides of slowly varied parity-time (PT) symmetry support localized optical resonances. The resonance is closely related to the formation of exceptional points separating exact and broken PT phases. Salient features of this kind of non-Hermitian resonance, including the formation of half-vortex flux and the discrete nature, are discussed. This investigation highlights the unprecedented uniqueness of field dynamics in non-Hermitian systems with many potential adaptive applications.

Keywords: resonance; exceptional points; parity-time symmetry; quantum optics.

DOI: 10.3788/COL202119.073601

1. Introduction

In the past decade, we have witnessed the great advances of parity-time (PT) symmetry of non-Hermitian quantum physics[1–10]. Among the many unique features of PT symmetry, exceptional points (EPs)[11–21] have attracted especial attention in the optical society. Unlike the diabolic points in Hermitian systems, EPs refer to the branch point singularities where both the eigenvalues and eigenvectors simultaneously coalesce. As the transition point separating the exact PT phase of real eigenvalues and the broken PT phase of complex solutions, an EP produces many interesting effects such as the coherent optical absorption, unidirectional reflectionlessness, and enhanced sensitivity[19].

From the non-Hermitian quantum theory, EPs are shown to satisfy the self-orthogonality condition[17]. An astonishing consequence of this condition is the stopped-light effect in parallel waveguides (WGs)[17,18]. Established in a totally different framework, this effect contributes to our understanding about slow-light science in Hermitian systems such as electromagnetically induced transparency, defective photonic crystals, and coupled ring resonators[22–24]. Nevertheless, there remain many unresolved questions. For example, former investigations only discussed the scenario in WGs of homogeneous PT symmetry[17]. The dynamics of the optical field in a slowly varying inhomogeneous PT-symmetric system with regions of broken and exact PT phases has not been discussed.

In this Letter, we investigate the field dynamics in inhomogeneous PT symmetric systems. We pay attention to a two-parallel-WG configuration, where the PT phase varies continuously and slowly, and the region of the exact PT phase surrounded by two EPs can form a localized optical resonator. Many features of this localized non-Hermitian resonance are discussed, including its discrete nature and the formation of half-vortex flux inside. The difference of this non-Hermitian resonance from those in Hermitian systems[22–24] is discussed. Potential adaptive applications are expected.

2. Theory

A schematic of two PT symmetric WGs under investigation is shown in Fig. 1. One of the WGs (WG1) has a positive imaginary component in the refractive index $n = n_w + j\gamma$ ($\gamma > 0$) and provides proper loss. The other WG (WG2) is a gain medium with $n = n_w - j\gamma$.

To modulate the PT phase in the system, we can refer to the standard non-Hermitian operator of

$$\begin{bmatrix} \beta + ig & \kappa \\ \kappa & \beta - ig \end{bmatrix} \begin{bmatrix} \Psi_1 \\ \Psi_2 \end{bmatrix} = k_{\mathrm{PT}} \begin{bmatrix} \Psi_1 \\ \Psi_2 \end{bmatrix} \quad (1)$$

for coupled WGs at a given angular frequency ω[17]. In this equation, β is the propagating constant in each separate WG, g

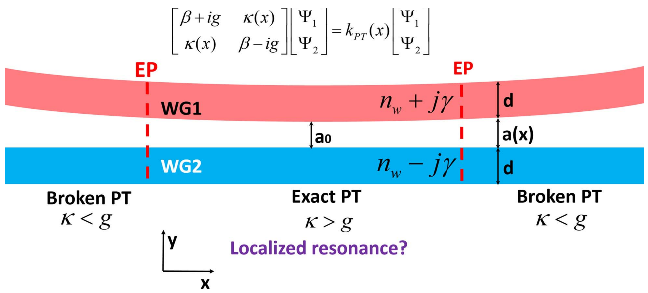

Fig. 1. Schematic of a two-WG inhomogeneous PT symmetric system in the x–y plane. When the PT phase changes very slowly, is it feasible to get a resonance in the exact PT region?

represents the gain/loss, κ is the mutual coupling strength, and Ψ_1 (Ψ_2) labels the field in WG1 (WG2). Because the PT phase is determined by the sign of $g^2-\kappa^2$, two schemes can be utilized in manipulating the PT phase. The first one is to change the gain/loss coefficient g related to the magnitude of γ. The second one is to control the mutual coupling coefficient κ by changing the distance a between the two WGs. Here, in order to provide an in-principle demonstration and by considering the feasibility of future experiments, we would adopt the second approach by assuming that the inter-WG distance a smoothly varies between the two WGs. All of the other parameters, including the refractive index $n_w \pm j\gamma$ and the WG width b, are kept constant. Note that Eq. (1) is usually utilized to describe the eigenvalues and eigenvectors of a homogenous system. However, if $a(x)$ varies sufficiently slowly, the mutual coupling strength $\kappa(x)$ can be handled as a locally invariant parameter. Now, Eq. (1) can still provide an accurate description of the eigenvalues and eigenvectors at any position of the system. The field would evolve adiabatically inside the inhomogeneous PT symmetric WGs.

3. Simulation and Analysis

To investigate the field dynamics in the spatial-varying PT system, we would like to utilize the full-wave numerical simulation software of COMSOL Multiphysics 5.4. The width d of each WG is 220 μm, and the interval between the two WGs is slowly changed following a third-order Bezier curve so that the minimum distance a_0 at the center of the structure ($x = 0$) equals 205 μm, and, at a distance of $x = 75$ mm away, the distance $a(x)$ is 468 μm. The refractive indices of WGs are $2.5 \pm 0.05j$, and other media are all air. Perfect matched layers (PMLs) are set around the structure to absorb the outward waves (we also verify that the scattering boundary condition and the periodic boundary condition give similar results as those shown in this Letter). The field is excited in the two WGs at $x = 0$ by using two z-directional currents (1 A) with identical phases placed. We also change the phase difference between the two currents and still obtain similar results, as presented below.

The COMSOL simulation shows that the region of exact PT phase can form a resonator. Figure 2 displays the results at two different frequencies of 227 GHz and 215 GHz, respectively. We can see that the field is localized and resonant around the location of minimum distance a, where the PT phase is conserved (exact PT). Nodes and peaks can be clearly observed in the field patterns. The geometric size of the resonance in the x direction increases when the frequency f decreases, which can be explained by the fact that, at a smaller frequency f (a larger wavelength λ), the field is less confined in the WGs, and the mutual coupling strength κ would increase. As a result, the PT broken region is pushed toward regions with a larger inter-WG distance a.

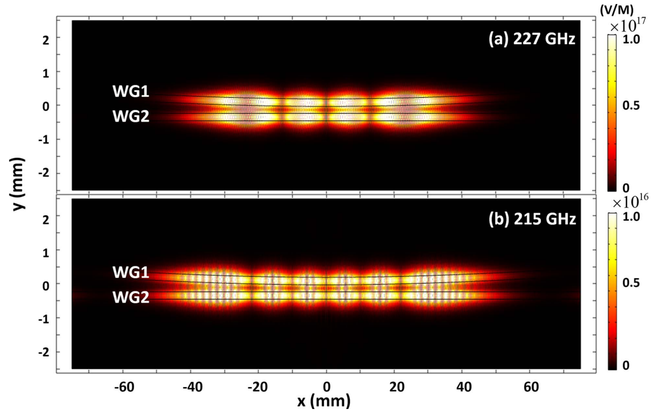

Fig. 2. Distribution of field amplitude E_z at the frequencies of (a) 227 GHz and (b) 215 GHz, respectively.

To provide more information about the physical mechanism of the localized resonance, we calculate the eigenvalues k_{PT} of the transverse electrical mode with a nonzero E_z component. The eigenvalues can be found from the full Maxwell's equations and the boundary conditions, which give

$$\mathfrak{R}_+\mathfrak{R}_- - \frac{(\beta+i\alpha_+)}{(\beta-i\alpha_+)}\frac{(\beta+i\alpha_-)}{(\beta-i\alpha_-)}e^{-4\beta_m a} = 0, \tag{2}$$

where

$$\mathfrak{R}_\pm = \frac{(\beta+i\alpha_\pm)^2\exp(i2\alpha_\pm b) - (\beta-i\alpha_\pm)^2}{(\beta-i\alpha_\pm)^2(e^{i2\alpha_\pm b}-1)}. \tag{3}$$

Here, $\beta^2 = k_{\mathrm{PT}}^2 - k_0^2$, $\alpha_\pm^2 = \varepsilon_\pm k_0^2 - k_{\mathrm{PT}}^2$, and $k_0^2 = \omega^2/c^2$. The solution of $\mathfrak{R}_\pm = 0$ determines the eigenmodes in each separate WG, and the last term of Eq. (1) represents the contribution from the inter-WG coupling.

The solutions of Eq. (2) at 227 GHz are shown in Fig. 3(b), together with the distribution of field amplitude E_z obtained from the COMSOL simulation [Fig. 3(a)]. The results for 215 GHz are similar to Fig. 3 and will not be discussed here. From Fig. 3, we can see that the localized resonance briefly occupies the region of exact PT phase supporting two real eigensolutions k_{PT}. This region can be understood as a non-Hermitian resonator. We also fit Fig. 3(b) by using Eq. (1) and find that $\beta = 1.95\ \mathrm{mm}^{-1}$ and $\kappa = 0.07\ \mathrm{mm}^{-1}$ when $x = 0$ mm, and that $\kappa = 0.009\ \mathrm{mm}^{-1}$ when $x = 75$ mm. κ is always much smaller than β. The relative variation of κ with respect to β is $\Delta\kappa/\beta =$

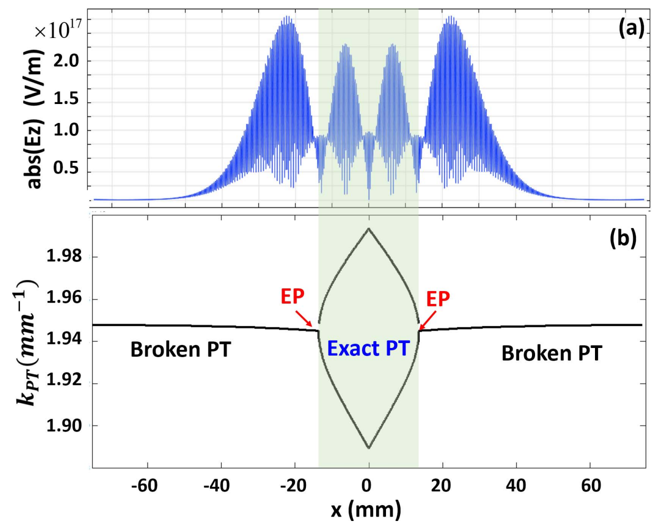

Fig. 3. (a) Distribution of field amplitude from the COMSOL simulation at 227 GHz. (b) The calculated real part of k_{PT} in the structure. At the central of the structure, the PT phase is exact, while across EPs, the PT phase is broken.

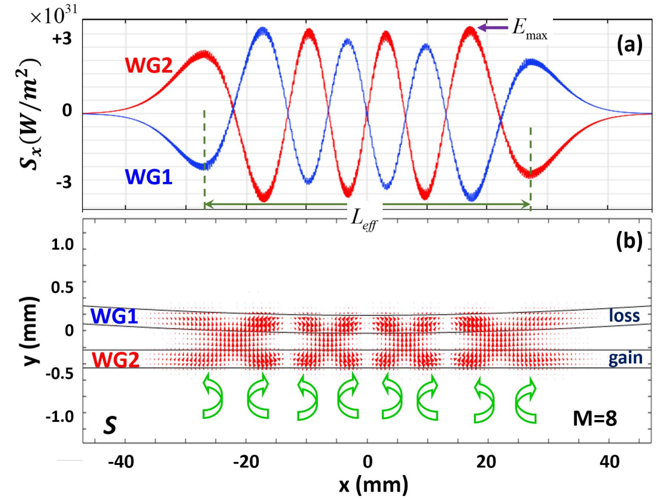

Fig. 4. (a) Distribution of energy flux S_x inside the two WGs at 227 GHz. (b) Distribution of the two-dimensional energy flux in the xy plane. Green arrows (with a number of $M = 8$) at the lower blank space represent the direction of energy flux in the coupled WGs.

3.1% from $x = 0$ mm to $x = 75$ mm or, in other words, 2.2×10^{-4} per wavelength. The mutual coupling strength κ indeed varies very slowly inside the structure.

The physical mechanism of the localized resonance must be attributed to the complex field dynamics of the non-Hermitian system. We believe that the main factor comes from the impedance mismatching between the broken PT phase (complex solution of $k_{\mathrm{PT}} = k_b + jk_i$) and the exact PT region (including EP) with real eigensolution $k_{\mathrm{PT}} = k_e$. The value of $R = |(k_b - k_e + jk_i)/(k_b + k_e + jk_i)|^2$ that usually represents the reflection coefficient of waves is clearly nonzero. With increased imaginary component k_i when the wave propagates deeper inside the broken PT region, the accumulated impedance-mismatching effect may produce a strong backward reflection that finally determines the formation and size of the non-Hermitian resonance. The stopped-light effect at EPs also helps to reflect the incident wave backward. Note that Fig. 3 implies that the field still penetrates into the broken PT phase region and finally decays away. The nonzero field in the broken-PT region can be explained by the non-unity value of R and the adiabatically varied parameters in the coupled WG system, the latter of which cannot forbid the tunneling effect. A detailed analysis on the physical mechanism of the above effect deserves our future attention.

The distribution of energy flux S in the non-Hermitian resonator is also studied. Figure 4(a) shows the distribution of S_x at the cores of the two WGs. We can see that the energy flux S_x in each separated WG can be either positive (forward propagation) or negative (backward propagation). Since S_x in the two WGs reverses their directions periodically and is always opposite to each other, we check whether vortices of energy flux are formed inside the whole system. However, when the two-dimensional energy flux is calculated, only half-vortices of energy flux can be observed, see Fig. 4(b). The energy flux forms arcs that begin from the gain medium (WG2) and end in the loss medium (WG1). Backward energy flux is absent. Such a kind of half-vortex cannot be observed in classic WGs and resonances and is a unique effect in the non-Hermitian WGs discussed here.

It is well known that resonance not only requires mirrors with high reflectivity, but also asks for coherent conditions on the accumulated phase after a round trip. As a result, resonance is usually discrete and can be characterized by a Q factor of $Q = \omega/\Delta\omega$, where $\Delta\omega$ is the full-width at half-maximum (FWHM) of the resonant peak. From Fig. 2, we can see that the resonances at the two different frequencies of 227 GHz and 215 GHz have different field magnitudes, so we test the variation of field amplitude versus the dipole frequency f. Similar to the definition of Q, we define the quality of the non-Hermitian resonance by the maximum amplitude $E_{\max}$ of E_z as defined in Fig. 4(a). Figure 5(a) shows the variation of $E_{\max}$ versus f. We can see at some discrete frequencies that the resonance is extremely strong. Within the frequency regime shown in Fig. 5(a), values of $E_{\max}$ can differ by up to two orders, representing a difference in the field intensity I by four orders.

The order of the discrete resonance can be defined by the number of half-vortices inside. For example, the resonance shown in Fig. 4(b) has an order M of eight. By analyzing the number of half-vortices at these discrete resonances, we find that M is different by a number of two between two adjacent resonances. The results are labeled in Fig. 5(a). Furthermore, from Fig. 2, we can see that the geometric size of the resonance varies with f, which is related to the shifted EPs in the inhomogeneous PT WGs. To characterize this effect, we define the effective resonator length L_{eff} as the distance of the peaks at two sides of the resonance [see Fig. 4(a)]. Figure 5(b) shows the variation of L_{eff} versus frequency f. We can see that it decreases monotonously with f, which is in agreement with the decreased mutual

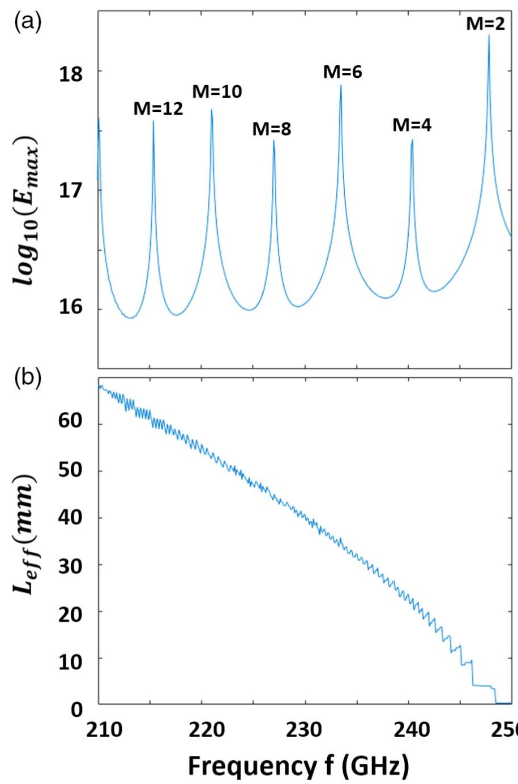

Fig. 5. (a) Maximum field E_{max} and (b) the effective resonator length L_{eff} versus f.

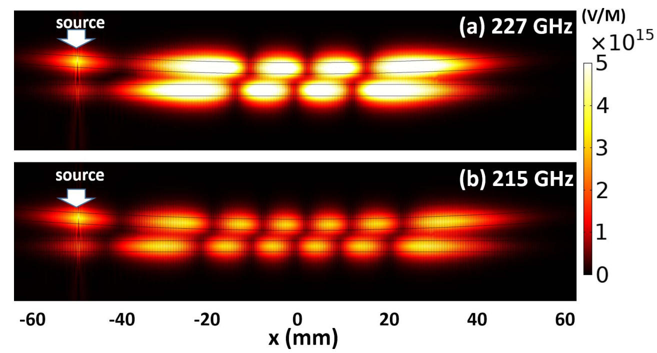

Fig. 6. Source being placed outside the PT symmetric region can still excite the non-Hermitian resonances at (a) 227 GHz and (b) 215 GHz.

coupling strength κ versus f. When f is greater than 250 GHz, no resonance is supported, because κ is always smaller than g.

Although the curve of Fig. 5(a) is very similar to the transmittance of an ordinary Fabry–Perot resonator, the non-Hermitian resonance discussed in this Letter is different from Fabry–Perot resonances because the effective resonator length L_{eff} varies with the frequency. Furthermore, the distribution of field is not homogenous [see Fig. 3(a)], and the field amplitudes in adjacent antinodes are not equal, which can be explained by the spatially varied PT phase. Then, it is an interesting question as to whether the non-Hermitian resonance can be excited with a field source being placed outside the PT symmetric region.

We perform COMSOL simulation and prove this feasibility, as shown in Fig. 6. Compared with Fig. 2, we can see that the field distribution shown in Fig. 6 is no longer symmetric with respect to the center of the WGs because the source is placed only at the left side of the PT symmetric region. Nevertheless, Fig. 6 proves unambiguously that the non-Hermitian resonance can be excited by outside excitation. Furthermore, the excited field at 227 GHz is stronger than that at 215 GHz, which is in good agreement with the results of Fig. 2, because the former one corresponds to the discrete resonance of $M = 8$.

4. Discussion

Above we provide adequate evidence on the existence of localized resonance in an inhomogeneous PT system. We also study the scenarios in some other configurations, including two straight WGs with spatially varied gain/loss, and two curved WGs that are symmetric with respect to the x axis. The phenomena discussed in this Letter are still obtained. So, the non-Hermitian resonance is a universal effect that relies only on the formation of EPs.

With the above analysis, we can see that the non-Hermitian resonance is different from other kinds of ordinary resonances[22–24]. Firstly, in classic systems within the Hermitian framework, a resonator requires high reflectivity from boundaries. The high reflectivity can be obtained by properly misaligned band gaps that forbid propagating modes outside the cavity or by high impedance mismatch at a sharp boundary. In sharp contrast, the non-Hermitian resonance presented in this Letter is excited in a seemingly open inhomogenous PT system with continuously and adiabatically changed parameters. No sharp boundary exists. Secondly, the non-Hermitian resonance is closely related to the transition between broken and exact PT phases via distributed loss and gain transverse to the propagating direction x of the field. In ordinary resonance, the modulation in the refractive index is usually along the x direction, e.g., sharp boundaries or Bragg gratings. Thirdly, at the discrete resonances of the inhomogenous PT system, we show that the half-vortices of energy flux are excited. In ordinary resonance, the vortices are always full. With the above mentioned merits, we believe that although the non-Hermitian resonance might not provide a giant Q factor as the ordinary resonance, e.g., in the Fabry–Perot resonator or the micro-cavity, it still contributes largely to the advances of our knowledge about slow/stopped light and resonant physics[22–24].

For future experiments, we can firstly fabricate two geometrically identical WGs (such as the cores of optical fibers) with proper gain and loss and then artificially displace them. As for potential applications, it is worth paying attention to the adaptive applications related to the self-determined geometric feature of the resonance. At different operational frequencies, the localized resonances could choose their own spatial regions (including the geometric size) in the inhomogeneous PT system. Various linear and nonlinear applications can be imaged. Future investigation could pay attention to revealing the unsolved issues of the non-Hermitian resonance, e.g., how to model the field dynamics by using the transfer matrix method and how to explain the phenomena in the broken PT region.

Before ending this Letter, we would like to emphasize other reported resonant features of PT symmetric systems. In fact, spontaneous emission at EPs and the associated density of states (DOS) have been discussed by various groups[13,25]. It is not a surprise that spontaneous emission can be enhanced at EPs since it supports stopped light, which is equivalent to the existence of a giant DOS. The giant DOS also explains the enhanced sensing performance of EPs[15,16,26]. Our investigation presented here is obviously different from these literatures about DOS at EPs, because EPs only occupy some discrete spatial point positions of the configuration shown in Fig. 1. The localized PT resonator is also different from those in reported literatures about EP-associated lasers[27–29]. The behavior of the field in the limit of infinitely slow parameter variation in PT systems has also been studied[30–33], but these literatures only consider the scenarios when encircling EPs.

5. Conclusion

In summary, paying attention to coupled WGs with slowly varying PT symmetry, we show that localized resonance can be achieved in the region of exact PT phase. We show that the non-Hermitian resonance is discrete in frequency, and the order of resonance can be defined by the number of half-vortices inside that run from the gain WG to the loss WG. The physical mechanism is briefly discussed. This investigation highlights the unprecedented uniqueness of field dynamics in non-Hermitian systems with many potential adaptive applications[34].

Acknowledgement

This work was supported by the National Natural Science Foundation of China (NSFC) (No. 11874228).

†These authors contributed equally to this work.

References

1. C. M. Bender, "Making sense of non-Hermitian Hamiltonians," Rep. Prog. Phys. **70**, 947 (2007).
2. S. Longhi, "PT-symmetric laser absorber," Phys. Rev. A **82**, 031801(R) (2010).
3. A. A. Zyablovsky, A. P. Vinogradov, A. V. Dorofeenko, A. A. Pukhov, and A. A. Lisyansky, "Causality and phase transitions in PT-symmetric optical systems," Phys. Rev. A **89**, 033808 (2014).
4. M. Lawrence, N. Xu, X. Zhang, L. Cong, J. Han, W. Zhang, and S. Zhang, "Manifestation of PT symmetry breaking in polarization space with terahertz metasurfaces," Phys. Rev. Lett. **113**, 093901 (2014).
5. J. Gear, F. Liu, S. T. Chu, S. Rotter, and J. Li, "Parity-time symmetry from stacking purely dielectric and magnetic slabs," Phys. Rev. A **91**, 033825 (2015).
6. W. Wang, L. Q. Wang, R. D. Xue, H. L. Chen, R. P. Guo, Y. Liu, and J. Chen, "Unidirectional excitation of radiative-loss-free surface plasmon polaritons in PT-symmetric systems," Phys. Rev. Lett. **119**, 077401 (2017).
7. S. Assawaworrarit, X. Yu, and S. Fan, "Robust wireless power transfer using a nonlinear parity-time-symmetric circuit," Nature **546**, 387 (2017).
8. H. Shen, B. Zhen, and L. Fu, "Topological band theory for non-Hermitian Hamiltonians," Phys. Rev. Lett. **120**, 146402 (2018).
9. L. Feng, R. El-Ganainy, and L. Ge, "Non-Hermitian photonics based on parity-time symmetry," Nat. Photo. **11**, 752 (2017).
10. R. El-Ganainy, K. G. Makris, M. Khajavikhan, Z. H. Musslimani, S. Rotter, and D. N. Christodoulides, "Non-Hermitian physics and PT symmetry," Nat. Phys. **14**, 11 (2018).
11. W. D. Heiss and H. L. Harney, "The chirality of exceptional points," Eur. Phys. J. D **17**, 149 (2001).
12. H. Cao and J. Wiersig, "Dielectric microcavities: model systems for wave chaos and non-Hermitian physics," Rev. Mod. Phys. **87**, 61 (2015).
13. Z. Lin, A. Pick, M. Loncar, and A. W. Rodriguez, "Enhanced spontaneous emission at third-order Dirac exceptional points in inverse-designed photonic crystals," Phys. Rev. Lett. **117**, 107402 (2016).
14. M. Kang, J. Chen, and Y. D. Chong, "Chiral exceptional points in metasurfaces," Phys. Rev. A **94**, 033834 (2016).
15. H. Hodaei, A. U. Hassan, S. Wittek, H. Garcia-Gracia, R. El-Ganainy, D. N. Christodoulides, and M. Khajavikhan, "Enhanced sensitivity at higher-order exceptional points," Nature **548**, 187 (2017).
16. W. Chen, S. K. Ozdemir, G. Zhao, J. Wiersig, and L. Yang, "Exceptional points enhanced sensing in an optical microcavity," Nature **548**, 192 (2017).
17. T. Goldzak, A. A. Mailybaev, and N. Moiseyev, "Light stops at exceptional points," Phys. Rev. Lett. **120**, 013901 (2018).
18. S. A. H. Gangaraj and F. Monticone, "Topological waveguiding near an exceptional point: defect-immune, slow-light, and loss-immune propagation," Phys. Rev. Lett. **121**, 093901 (2018).
19. M. A. Miri and A. Alu, "Exceptional points in optics and photonics," Science **363**, eaar7709 (2019).
20. Y. Li and C. Argyropoulos, "Exceptional points and spectral singularities in active epsilon-near-zero plasmonic waveguides," Phys. Rev. B **99**, 075413 (2019).
21. H. Z. Chen, T. Liu, H. Y. Luan, R. J. Liu, X. Y. Wang, X. F. Zhu, Y. B. Li, Z. M. Gu, S. J. Liang, H. Gao, L. Lu, L. Ge, S. Zhang, J. Zhu, and R. M. Ma, "Revealing the missing dimension at an exceptional point," Nat. Phys. **16**, 571 (2020).
22. J. B. Khurgin and R. S. Tucker, *Slow Light: Science and Applications* (CRC Press, 2009).
23. J. B. Khurgin, "Slow light in various media: a tutorial," Adv. Opt. Photon. **2**, 287 (2010).
24. L. Singh and W. Zhang, "Advancements in high refractive index media: from quantum coherence in atomic systems to deep sub-wavelength coupling in metamaterials," Chin. Opt. Lett. **18**, 062401 (2020).
25. A. Pick, B. Zhen, O. D. Miller, C. W. Hsu, F. Hernandez, A. W. Rodriguez, M. Soljacic, and S. G. Johnson, "General theory of spontaneous emission near exceptional points," Opt. Express **25**, 12325 (2017).
26. J. Wiersig, "Sensors operating at exceptional points: general theory," Phys. Rev. A **93**, 033809 (2016).
27. J. Zhang, B. Peng, S. K. Ozdemir, K. Pichler, D. O. Krimer, G. Zhao, F. Nori, Y. X. Liu, S. Rotter, and L. Yang, "A phonon laser operating at an exceptional point," Nat. Photon. **12**, 479 (2018).
28. Z. Zhang, X. Qiao, B. Midya, K. Liu, J. Sun, T. Wu, W. Liu, R. Agarwal, J. M. Jornet, S. Longhi, N. M. Litchinitser, and L. Feng, "Tunable topological charge vortex microlaser," Science **368**, 760 (2020).
29. H. Hodaei, M. Ali Miri, M. Heinrich, D. N. Christodoulides, and M. Khajavikhan, "Parity-time-symmetric microring lasers," Science **346**, 975 (2014).
30. B. Longstaff and E. M. Graefe, "Nonadiabatic transitions through exceptional points in the band structure of a PT-symmetric lattice," Phys. Rev. A **100**, 052119 (2019).
31. M. V. Berry and R. Uzdin, "Slow non-Hermitian cycling: exact solutions and the Stokes phenomenon," J. Phys. A **44**, 435303 (2011).
32. E. M. Graefe, A. A. Mailybaev, and N. Moiseyev, "Breakdown of adiabatic transfer of light in waveguides in the presence of absorption," Phys. Rev. A **88**, 033842 (2013).
33. T. J. Milburn, J. Doppler, C. A. Holmes, S. Portolan, S. Rotter, and P. Rabl, "General description of quasiadiabatic dynamical phenomena near exceptional points," Phys. Rev. A **92**, 052124 (2015).
34. Y. Jia and F. Chen, "Compact solid-state waveguide lasers operating in the pulsed regime: a review," Chin. Opt. Lett. **17**, 012302 (2019).